Industrial Crops & Products 231 (2025) 121195

Contents lists available at ScienceDirect

Industrial Crops & Products

journal homepage: www.elsevier.com/locate/indcrop

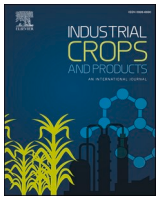

Differences in the content, composition and structure of the native-like lignins in leucaena and tagasaste shrubs for biorefinery applications

Mario J. Rosado [a], Jorge Rencoret [a], Ana Gutiérrez [a], Manuel J. Díaz [b], José C. del Río [a,*]

[a] Instituto de Recursos Naturales y Agrobiología de Sevilla, CSIC, Avda. Reina Mercedes, 10, Seville 41012, Spain
[b] PRO2TECS, Chemical Engineering Department, "El Carmen" Campus, University of Huelva, Huelva, Spain

ARTICLE INFO

Keywords:
Leucaena
Tagasaste
Lignin
Guaiacyl
Syringyl
Biorefineries

ABSTRACT

Leucaena and tagasaste are fast-growing leguminous shrubs recognized for producing substantial amounts of lignocellulosic biomass, making them promising candidates as alternative feedstocks for biorefineries. However, despite extensive research into their chemical composition, a detailed understanding of their native lignin structure remains limited, hindering their optimal use in lignocellulosic biorefineries. In this study, native-like lignins were isolated and thoroughly analyzed using a variety of analytical techniques, including gel permeation chromatography (GPC), analytical pyrolysis coupled to gas chromatography/mass spectrometry (Py-GC/MS), two-dimensional Nuclear Magnetic Resonance (2D NMR), and ^{31}P NMR. The data revealed significant differences in the lignin composition of the two species. Leucaena lignin showed a strong predominance of guaiacyl (G) units, with minor amounts of syringyl (S), and *p*-hydroxyphenyl (H) units (H:G:S ratio of 1:83:16; S/G 0.19). In contrast, tagasaste lignin exhibited a slight predominance of S units (H:G:S ratio of 2:46:52; S/G 1.13). These compositional variations significantly influenced the distribution of the different lignin interunit linkages. Hence, leucaena lignin was characterized by fewer of β–*O*–4′ alkyl-aryl ether linkages (66 % of all linkages) and a higher proportion of condensed linkages, making it more resistant to delignification. In contrast, tagasaste lignin presented higher levels of β–*O*–4′ alkyl-aryl ether linkages (74 %) and fewer condensed linkages, rendering it more susceptible to delignification. The insights gained from this study are expected to enhance the valorization of these lignocellulosic materials as feedstocks in future lignocellulosic biorefineries.

1. Introduction

The transition to renewable energy and sustainable materials is essential for the development of modern societies and the mitigation of climate change. Plant biomass, the most abundant renewable resource on Earth, offers great potential as a basis for producing renewable energy and biobased products. Replacing fossil fuels with biomass can reduce our reliance on finite fossil fuel reserves and significantly reduce anthropogenic net CO_2 emissions (Yang et al., 2021). Biomass is widely available from forest, agricultural and industrial lignocellulosic wastes, making it a valuable resource for producing biofuels and bioproducts, paving the way for reduced carbon emissions, enhanced energy security, and fostering a circular bioeconomy (Ragauskas et al., 2006). A central concept in this transition is the lignocellulose biorefinery, which enables the conversion of renewable plant biomass into energy and diverse products in an economically and environmentally sustainable manner (Kamm et al., 2008; Ubando et al., 2020; Vinod et al., 2020; Liu et al., 2021; Lago et al., 2019; Nunes et al., 2020). This has stimulated interest in identifying high-yield biomass crops suitable for such lignocellulosic biorefineries.

In this study, we examined two fast-growing leguminous shrubs, leucaena (*Leucaena leucocephala* L.) and tagasaste (*Chamaecytisus proliferus* spp. *palmensis* L.), both members of the Fabaceae family. Leguminous plants are essential to sustainable agriculture due to their symbiotic relationship with *Rhizobium* bacteria, which enables atmospheric nitrogen fixation (Jensen et al., 2012; Wu et al., 2017; Stagnari et al., 2017). This natural process reduces dependency on synthetic fertilizers and enhances soil fertility for subsequent crops. Beyond their role in agriculture, legumes such as leucaena and tagasaste hold great promise as feedstocks for lignocellulosic biorefineries, producing biofuels, biomaterials, and biochemicals (Jensen et al., 2012). These species thrive in degraded soils, improve microbial activity, control erosion, and reduce soil acidity, contributing to ecosystem restoration (McKenzie et al., 2001; Loaiza et al., 2018; Monjardino et al., 2010;

* Corresponding author.
E-mail address: delrio@irnase.csic.es (J.C. del Río).

https://doi.org/10.1016/j.indcrop.2025.121195
Received 20 January 2025; Received in revised form 3 April 2025; Accepted 10 May 2025
Available online 14 May 2025

Rodríguez-Echevarría et al., 2003). Both species are highly productive, with leucaena capable of yielding over 50 tons of biomass per hectare annually, increasing to approximately 70 tons after seven years (Feria et al., 2012; Loaiza et al., 2017). Tagasaste, although less prolific, can produce around 18.3 tons per hectare per year (González, 2000). These high yields, coupled with their adaptability and soil-enhancing properties, make them attractive candidates for biorefinery feedstocks. Additionally, they show potential for applications such as paper pulp production, hemicellulose recovery, and lignocellulosic nanofiber production (Jiménez et al., 2007; Alfaro et al., 2010; Espinosa et al., 2017; Domínguez-Robles et al., 2017, 2020; García et al., 2008; López et al., 2004; Palma et al., 2021).

Despite extensive research on the chemical composition of leucaena and tagasaste, detailed information on the structure of their native lignins remains limited. Lignin is a complex and heterogeneous polymer that provides structural support, enhances water transport, and reinforces plant defense against pathogens. Structurally, lignin consists of three primary units, *p*-hydroxyphenyl (H), guaiacyl (G), and syringyl (S) units, resulting from the polymerization of the monolignols *p*-coumaryl, coniferyl, and sinapyl alcohols (Vanholme et al., 2010; Ralph et al., 2019). Lignin biosynthesis involves the oxidation of the monolignols, catalyzed by peroxidases and laccases, followed by combinatorial radical coupling, resulting in a structurally complex polymer that lacks regular, ordered repeating units, making it particularly recalcitrant and strongly limiting plant cell-wall degradability (Vanholme et al., 2010; Ralph et al., 2019).

This study aims to provide a comprehensive characterization of the native lignins in tagasaste and leucaena. To achieve this, native-like lignins were isolated using classical methods and analyzed using advanced analytical techniques such as gel permeation chromatography (GPC), pyrolysis-gas chromatography/mass spectrometry (Py-GC/MS), two-dimensional Nuclear Magnetic Resonance (2D NMR)' and ^{31}P NMR. The insights obtained are expected to enhance the understanding of these lignocellulosic materials, facilitating their optimized utilization in biorefineries and expanding their potential as sustainable feedstocks for bio-based industries.

2. Materials and methods

2.1. Samples and analysis of the main constituents

Leucaena (*Leucaena leucocephala* L.) and tagasaste (*Chamaecytisus proliferus* spp. *palmensis*) were cultivated in an experimental field in Huelva (Spain). The harvested samples were air-dried and milled in an IKA MF 10 knife mill (IKA, Staufen, Germany) to pass through 1 mm screen. Milled samples were extracted sequentially with acetone (8 h), methanol (8 h), and hot water (8 h) using a Soxhlet apparatus. Extractives were quantified gravimetrically by evaporating the solvents using a rotary evaporator. The total lignin content was determined by summing the Klason lignin and acid-soluble lignin fractions. Klason lignin was determined by hydrolyzing the pre-extracted lignocellulosic material with H_2SO_4, while acid-soluble lignin was measured spectrophotometrically at 205 nm, according to the Tappi methods T222 om-88 and UM 250, respectively (Tappi, 2004). The holocellulose fraction (comprising hemicelluloses and cellulose) was determined from pre-extracted materials using the acid chlorite method (Browning, 1967). Cellulose content was measured by selectively removing the hemicelluloses from the holocellulose through alkaline extraction (Browning, 1967). Ash content was measured gravimetrically by incinerating the samples at 575 ºC for 6 h. All analyses were performed in triplicate. The means were compared by using the *t*-test or one-way ANOVA and Tukey's test ($p > 0.05$) for multiple comparisons between the two lignocellulosic materials.

2.2. Isolation and purification of the lignin fraction

Approximately 60 g of pre-extracted samples were processed in a Retsch PM-100 planetary mill (Retsch, Haan, Germany), using an agate jar and balls at a rotation speed of 400 rpm for 16 h, alternating between 20 min of milling time and 10 min of rest. The milled material was then extracted with a dioxane:water solution (90:10 v/v) for 16 h, and the solubilized lignin in the resulting supernatant was separated by centrifugation. This extraction procedure was repeated twice more, each time using fresh dioxane:water solution. The combined dioxane:water solutions were evaporated to dryness using a rotary evaporator at 40 ºC. The crude milled wood lignin (MWL) obtained was further purified as detailed elsewhere (del Río et al., 2012). The MWL yields in both samples accounted for around 20 % of the total lignin content (Klason lignin and acid-soluble lignin).

2.3. Gel Permeation Chromatography (GPC)

Prior to GPC analysis, the lignins were acetylated using a 1:1 (v/v) mixture of acetic anhydride and pyridine. The acetylated lignins were then dissolved in tetrahydrofuran and analyzed using a Shimadzu Prominence-i-LC-2030 3D GPC system (Shimadzu, Kyoto, Japan), under the experimental conditions detailed previously (Rencoret et al., 2018).

2.4. Analytical pyrolysis

Approximately 0.1 mg of MWLs were subjected to pyrolysis at 500 °C for 1 min using a EGA/PY-3030D microfurnace pyrolyzer (Frontier Laboratories Ltd., Fukushima, Japan) coupled to an Agilent 7820 A GC and an Agilent 5975 mass selective detector (Agilent Technologies, Inc., Santa Clara, CA). The system was equipped with a DB-1701 column (30 m × 0.25 mm i.d., 0.25 μm film thickness). The oven temperature in the GC was initially set at 50 °C for 1 min, then ramped to 100 °C at a rate of 30 °C min^{-1}, and then raised to 280 °C at a rate of 6 °C min^{-1}, and held for 10 min. Released compounds were identified by comparing their mass spectra against a collection of standards, the NIST mass spectra database, and literature data (Ralph and Hatfield, 1991; del Río et al., 2005). For each compound, the molar peak areas were normalized, and the results, expressed as percentages, were averaged over two replicates.

2.5. 2D NMR spectroscopy

The 2D NMR analyses were conducted on a Bruker Avance III 500 MHz spectrometer (Bruker, Karlsruhe, Germany) equipped with a 5 mm TCI cryoprobe. Approximately 40 mg of MWLs were dissolved in 0.6 mL of DMSO-d_6. Heteronuclear Single Quantum Coherence (HSQC) spectra were acquired using the standard "hsqcetpgsisp.2.2" pulse program and the parameters previously described (del Río et al., 2012). Signal assignments were based on comparisons with established literature (del Río et al., 2012; Ralph et al., 2009; Rosado et al., 2023). For the semiquantitative analysis of the HSQC signals, Bruker's Topspin 4.2 software was used. Signal integration was done separately for the aliphatic oxygenated (linkages) and the aromatic/unsaturated regions, as described elsewhere (del Río et al., 2012). In the aromatic/unsaturated region of the spectrum, C_2/H_2 correlation signals were used to quantify the relative abundances of H, G and S lignin units. For the $S_{2,6}$ and $H_{2,6}$ signals, which correspond to two pairs of protonated carbons, the integration volumes were halved. In the oxygenated/aliphatic region of the spectrum, the relative abundances of side-chains involved in the different lignin linkages (**A**, **B**, **C**, **D**, **F**) were determined from the C_α/H_α correlations (A_α, B_α, C_α, D_α, and F_α signals), except for the cinnamyl alcohol end-groups (**I**), where C_γ/H_γ correlations (I_γ signal) were used. The relative abundance of cinnamaldehyde end-groups (**J**) was calculated by integrating the J_β signal and comparing it to the I_β signal.

2.6. ^{31}P NMR spectroscopy

Prior to the ^{31}P NMR analyses, approximately 30 mg of MWLs were subjected to a phosphtylation procedure with 2-chloro-4,4,5,5-tetramethyl-1,3,2-dioxaphospholane (TMDP), as previously indicated (Benito et al., 2024). The ^{31}P NMR spectra were acquired on a Bruker Avance NEO 400 MHz equipment (Bruker, Karlsruhe, Germany) using the pulse program "zgig", a relaxation delay of 5 s and 256 accumulated scans. Chemical shifts were calibrated with respect to the distinct signal from the hydroxylated-TMDP at 132.2 ppm. The signals in the ^{31}P NMR spectra were assigned based on the literature (Pu et al., 2011; Meng et al., 2019; Benito et al., 2024). The quantification of the hydroxyl groups was carried out using *N*-hydroxy-5-norbornene-2,3-dicarboximide (NHND) as an internal standard, following the method described in previous studies (Benito et al., 2024).

3. Results and discussion

3.1. Main constituents of leucaena and tagasaste

The composition of the main constituents of leucaena and tagasaste is summarized in Table 1. Overall, the results are similar to those reported previously (Díaz et al., 2004; López et al., 2010; Marques et al., 2008; Loaiza et al., 2018; Domínguez-Robles et al., 2020; Palma et al., 2021). Both species exhibited relatively low levels of extractives (acetone, methanol, and water-soluble), with leucaena containing up to 5.4 %, compared to only 3.8 % for tagasaste. Significant differences were observed in the holocellulose content, with leucaena having 69.1 % and tagasaste having a higher content of 77.5 %. These differences were mainly due to variations in hemicellulose content; leucaena contained only 29.6 % of hemicelluloses, while tagasaste presented a notably higher content of 39.5 %. The cellulose content of both species was comparable, with leucaena having 39.5 % and tagasaste containing 38.0 %. Both species also exhibited low ash content, with leucaena containing 1.3 % and tagasaste only 0.7 %. Finally, the total lignin content, comprising Klason lignin and acid-soluble lignin, varied considerably between the two species. Leucaena had a lignin content of 24.2 %, compared to only 18.0 % in tagasaste.

Since lignin is a highly recalcitrant polymer, its content plays a crucial role in determining biomass resistance to degradation. However, beyond the quantity of lignin, its composition is equally important for accurately assessing the overall recalcitrance of the lignocellulosic biomass. To examine the structure of the lignins in these species, native-like lignin preparations were isolated using aqueous dioxane extraction, following the traditional method (Björkman, 1956). This method produced lignin preparations with minimal structural alterations, thereby preserving the native lignin structure in the plant. The isolated lignins (commonly referred to as 'milled-wood lignins', MWL) were thoroughly analyzed using a combination of advanced techniques, such as GPC to measure molecular weights, Py-GC/MS to determine the composition of lignin units, 2D NMR spectroscopy to gain detailed insights into lignin units and their inter-unit linkages, and ^{31}P NMR, which provided information on the nature of both the aliphatic and phenolic hydroxyl groups.

Table 1
Abundance (%) of the main constituents of leucaena and tagasaste (values with the same letters in the same parameters indicate that the values did not differ by the Tukey test at 0.95 confidence interval).

	Leucaena	Tagasaste
Acetone extractives	1.8 ± 0.2a	1.4 ± 0.1a
Methanol extractives	2.1 ± 0.1a	1.9 ± 0.1a
Water-soluble extractives	1.5 ± 0.1c	0.5 ± 0.0a
Klason lignin	22.1 ± 0.4c	16.3 ± 0.1a
Acid-soluble lignin	2.1 ± 0.1b	1.7 ± 0.1a
Hemicelluloses	29.6 ± 1.0a	39.5 ± 1.3c
Cellulose	39.5 ± 1.0a	38.0 ± 1.5a
Ash	1.3 ± 0.1b	0.7 ± 0.1a

3.2. Molecular weight distribution of the lignins of leucaena and tagasaste as determined by GPC

The molecular weights of the MWLs from leucaena and tagasaste were analyzed using GPC, as illustrated in Fig. 1. The GPC analysis confirmed that the isolated MWLs are polymeric, ruling out the occurrence of low molecular weight compounds. The weight-average (M_w) molecular weight, number-average (M_n) molecular weight, and polydispersity indices (M_w/M_n) of these MWLs, obtained from the GPC, are presented in Table 2. The analysis indicated that the MWL from leucaena presented a M_w of 6160 g/mol and a M_n of 3450 g/mol, with a low polydispersity of 1.79, demonstrating a high level of homogeneity of this MWL. In comparison, the MWL from tagasaste exhibited a slightly higher molecular weight, with a M_w of 7880 g/mol and a M_n of 4000 g/mol, and a similarly low polydispersity of 1.97. These values are comparable to those reported for MWLs isolated from other hardwoods, including beech, eucalyptus, and orange tree prunings (Rosado et al., 2023; Brosse et al., 2010; Tolbert et al., 2014; H.M. Wang et al., 2017).

3.3. Lignin composition of leucaena and tagasaste as determined by Py-GC/MS

Leucaena and tagasaste MWLs were analyzed using Py-GC/MS, a thermal degradation technique that enables a rapid evaluation of lignin unit composition. Fig. 2 displays the Py-GC/MS chromatograms of both MWLs, while Table 3 lists the released phenolic compounds along with their relative molar abundances. The absence of carbohydrate-derived compounds in the pyrograms confirms the high purity and successful isolation of the MWL preparations. The pyrolysis predominantly released guaiacyl- (G) and syringyl- (S) derived compounds, including guaiacol (peak 2), 4-methylguaiacol (peak 5), 4-ethylguaiacol (peak 6), 4-vinylguaiacol (peak 7), eugenol (peak 8), *cis*-isoeugenol (peak 10), *trans*-isoeugenol (peak 11), and vanillin (peak 13), among others, as well as their corresponding S-derivatives. Phenolic compounds derived from H-lignin units, such as phenol (peak 1), 3-methylphenol (peak 3), and 4-methylphenol (peak 4), were also detected, though in smaller quantities. The significant presence of phenolic compounds with intact three carbon side chains (particularly peaks 8, 10, 11, 22, 24, and 27, among others) observed in the pyrograms indicates that the lignin structure was well-preserved during the MWL isolation process, with negligible structural

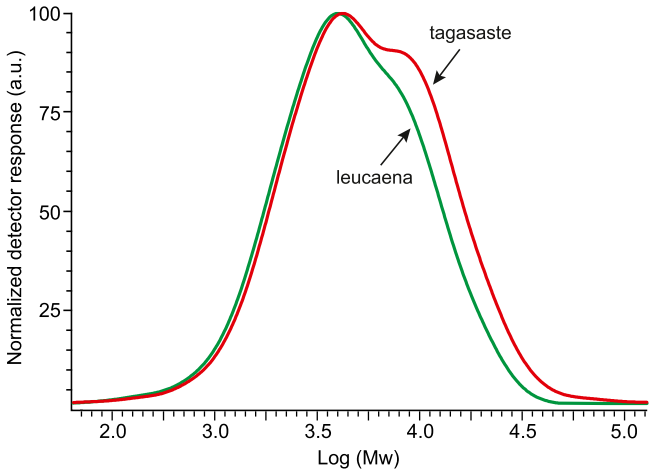

Fig. 1. GPC curves for the MWLs isolated from leucaena (green) and tagasaste (red). The weight-average (M_w) molecular weight, number-average (M_n) molecular weight, and polydispersity indices (M_w/M_n) for these MWLs are detailed in Table 2.

Table 2
Weight-average (M_w) and number-average (M_n) molecular weights (g mol^{-1}), and polydispersity (M_w/M_n) of the MWLs isolated from leucaena and tagasaste.

	Leucaena	Tagasaste
M_w	6160	7880
M_n	3450	4000
M_w/M_n	1.79	1.97

alterations (del Río et al., 2001, 2002).

Important differences were observed in the profiles of the phenolic compounds released from the two MWLs upon pyrolysis. The MWL from leucaena predominantly released phenolic compounds derived from G-lignin units, with fewer amounts of phenolic compounds derived from S-lignin units, while the MWL from tagasaste produced slightly higher amounts of S-lignin-derived phenolics. The lignin H:G:S ratio of the MWLs from both species was estimated based on the relative abundance of the phenolic compounds released during Py-GC/MS. The pyrolysis data revealed that the MWL from leucaena was predominantly enriched in G-lignin units, with an H:G:S ratio of 2:82:16 and an S/G ratio of 0.19. In contrast, the MWL from tagasaste showed a slightly higher predominance of S-lignin units, with an H:G:S ratio of 2:47:51 and an S/G ratio of 1.07, as shown in Table 3.

Structurally, G-units possess a free C5 position, allowing the formation of additional condensed carbon–carbon or ether linkages, resulting in a more branched and condensed lignin structure (Vanholme et al., 2010; Ralph et al., 2019). In contrast, S-lignin units lack a free *ortho* position, preventing the formation of 5–5′ and β–5′ linkages with the aromatic ring, leading to the preferential formation of β–*O*–4′ ether linkages, and resulting in a less branched and a more linear structure. The distinct lignin compositions in leucaena and tagasaste consequently influence the distribution of inter-unit linkages, as we will see below, which significantly affects their reactivity and the potential applications of their lignin in various biorefinery processes.

3.4. Lignin composition and inter-unit linkages as determined by 2D NMR

The MWLs from leucaena and tagasaste were further analyzed using 2D-HSQC NMR spectroscopy, which offers insights into both the

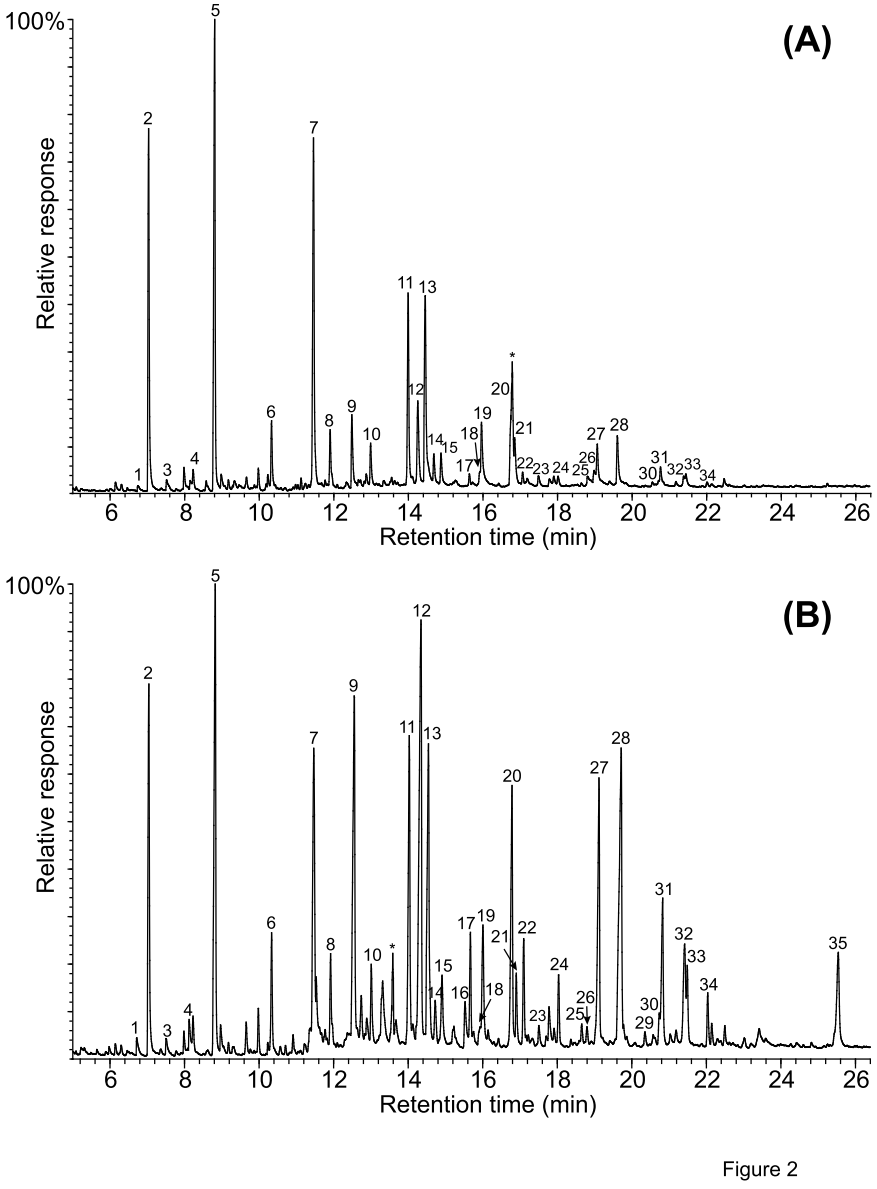

Figure 2

Fig. 2. Py-GC/MS of the MWLs isolated from leucaena (**A**) and tagasaste (**B**). The identities and relative abundances of the released numbered phenolic compounds are listed in Table 3.

Table 3
Identities and relative molar abundances (%) of the phenolic compounds released upon Py-GC/MS of the MWLs from leucaena and tagasaste.

Label	Compound	Origin	MWL leucaena	MWL tagasaste
1	phenol	H	0.6	0.6
2	guaiacol	G	15.8	7.2
3	3-methylphenol	H	0.9	0.5
4	4-methylphenol	H	0.6	0.8
5	4-methylguaiacol	G	19.9	9.7
6	4-ethylguaiacol	G	2.4	1.8
7	4-vinylguaiacol	G	14.9	6.4
8	eugenol	G	2.3	1.1
9	syringol	S	3.1	9.0
10	*cis*-isoeugenol	G	1.6	1.1
11	*trans*-isoeugenol	G	7.1	5.4
12	4-methylsyringol	S	3.7	11.9
13	vanillin	G	9.6	6.6
14	propyne-guaiacol	G	1.0	0.7
15	propyne-guaiacol	G	1.2	1.0
16	homovanillin	G	0.0	0.9
17	4-ethylsyringol	S	0.4	1.6
18	vanillic acid methyl ester	G	0.5	0.4
19	acetoguaiacone	G	3.4	2.1
20	4-vinylsyringol	S	2.3	4.6
21	guaiacylacetone	G	1.6	0.8
22	4-allylsyringol	S	0.4	1.4
23	propiovanillone	G	0.5	0.4
24	*cis*−4-propenylsyringol	S	0.3	1.0
25	propyne-syringol	S	0.1	0.3
26	propyne-syringol	S	0.1	0.3
27	*trans*−4-propenylsyringol	S	1.4	4.8
28	syringaldehyde	S	2.1	8.0
29	homosyringaldehyde	S	0.0	0.3
30	syringic acid methyl ester	S	0.2	0.4
31	acetosyringone	S	0.9	2.5
32	*trans*-coniferaldehyde	G	0.4	1.7
33	syringylacetone	S	0.5	1.2
34	propiosyringone	S	0.2	0.8
35	*trans*-sinapaldehyde	S	0.0	2.7
		H=	2.1	1.9
		G=	82.2	47.3
		S=	15.7	50.8
		S/G=	0.19	1.07

H: *p*-hydroxyphenyl units; G: guaiacyl units; S: syringyl units

composition of lignin units and the various inter-unit linkages. The HSQC spectra are presented in Fig. 3, while the identified lignin units and substructures are shown in Fig. 4. The spectra are divided into two regions, the aliphatic/oxygenated region (δ_C/δ_H 50–90/2.5–6.0), which offers insights into the inter-unit linkages, and the aromatic/unsaturated region (δ_C/δ_H 98–155/5.8–7.8), which provides information on the composition of H-, G-, and S-lignin units. The correlation signals observed in the HSQC spectra, along with their assignments, are summarized in Table 4.

The signals in the aromatic/unsaturated region of the HSQC spectra corroborated the Py-GC/MS data. Signals corresponding to S-, G-, and H-lignin units were observed. S-lignin units showed a strong correlation for the $C_{2,6}/H_{2,6}$ signal at δ_C/δ_H 103.7/6.68. Additionally, signals for the $C_{2,6}/H_{2,6}$ correlations of Cα-oxidized S-lignin units (S′) were detected at δ_C/δ_H 106.3/7.32 and 106.3/7.20. G-lignin units exhibited distinct correlation signals for C_2/H_2, C_5/H_5, and C_6/H_6, at δ_C/δ_H 110.8/6.96, 115.0/6.74, and 118.7/6.77. A signal for the $C_{2,6}/H_{2,6}$ correlations of H-lignin units was also observed at δ_C/δ_H 127.7/7.20, although at lower intensities, reflecting the small amounts of H-lignin units in both MWLs, consistent with the findings from the Py-GC/MS analysis.

The signals observed in the aliphatic/oxygenated region of the spectra provided valuable insights into the various lignin inter-unit linkages. In this region, alongside the methoxyl group signal, the most prominent signals corresponded to β–*O*–4′ alkyl–aryl ether linkages (A). The C_α/H_α correlations appeared at δ_C/δ_H 70.9/4.72 for β–*O*–4′ linkages associated with G-units and at δ_C/δ_H 71.9/4.85 for those linked to S-units, while the C_β/H_β correlations were found at δ_C/δ_H 83.7/4.26 for β–*O*–4′ linkages linked to G-unit and at δ_C/δ_H 85.8/4.09 for those linked to S-units. The C_γ/H_γ correlations for β–*O*–4′ linkages were observed at δ_C/δ_H 59.7/3.25 and 3.58. Additional signals from other lignin substructures were also present, including β–5′ phenylcoumarans (B), β–β' resinols (C), 5–5′ dibenzodioxocins (D), and β–1′ spirodienones (F), as well as cinnamyl alcohol end-groups. Among these, the most intense signals came from β–5′ phenylcoumarans (B), with their C_α/H_α and C_β/H_β correlations found at δ_C/δ_H 86.8/5.45 and 53.0/3.45, respectively, while their C_γ/H_γ correlations overlapped with other signals around δ_C/δ_H 62.5/3.67. Strong signals were also observed for β–β' resinols (C), showing C_α/H_α, C_β/H_β, and C_γ/H_γ correlations at δ_C/δ_H 84.8/4.66, 53.6/3.05, and 70.9/3.82 and 4.18, respectively. Clear signals for 5–5′ dibenzodioxocins (D) were detected in the spectra of both species, although they were more pronounced in the spectrum of the MWL of leucaena, with their C_α/H_α and C_β/H_β correlations at δ_C/δ_H 83.0/4.81 and 85.3/3.83. Additionally, small signals from β–1′ spirodienones (F) were visible in this part of the spectrum, characterized by their C_α/H_α, $C_{\alpha'}/H_{\alpha'}$, C_β/H_β, and $C_{\beta'}/H_{\beta'}$ correlations at δ_C/δ_H 81.0/5.09, 83.4/4.70, 59.7/2.74, and 79.3/4.11, respectively. Other signals for spirodienones, such as the $C_{2'}/H_{2'}$, $C_{5'}/H_{5'}$, $C_{6'}/H_{6'}$ correlations, were observed in the aromatic region of the spectra. Finally, a signal corresponding to the C_γ/H_γ correlations of *p*-hydroxycinnamyl alcohol (I) end-groups was observed at δ_C/δ_H 61.3/4.08; likewise, signals for the C_α/H_α, and C_β/H_β correlations were observed in the aromatic region of the spectra.

The relative abundances of the main lignin inter-unit linkages, *p*-hydroxycinnamyl end-groups, and lignin units in the MWLs isolated from leucaena and tagasaste were estimated from the 2D-HSQC NMR spectra and are summarized in Table 5. The NMR analysis revealed important differences in the composition of the lignins from the two species. The lignin of leucaena was predominantly composed of G-lignin units, making up 83 % of all aromatic units, with smaller amounts of S-lignin units (16 %) and only trace amounts of H-lignin units (1 %), resulting in an S/G ratio of 0.19. In contrast, the lignin from tagasaste exhibited a slight predominance of S-lignin units (52 %), followed by G-lignin units (46 %), and a small proportion of H-lignin units (2 %), with an S/G ratio of 1.13. These findings are consistent with the Py-GC/MS analysis shown above.

The differences in lignin composition between the two species significantly influenced the distribution of the various inter-unit linkages. In leucaena lignin, which was enriched in G-lignin units, there was a lower proportion of β–*O*–4′ alkyl-aryl ether linkages (66 % of all inter-unit linkages identified) and a higher content of condensed linkages, such as β–5′ phenylcoumarans (21 %) and 5–5′ dibenzodioxocins (4 %). The presence of significant amounts of dibenzodioxocins in leucaena lignin is particularly noteworthy, as these condensed structures are typically associated with softwood lignins, where they function as branching points (Karhunen et al., 1995; Ralph et al., 2019). Their important occurrence in leucaena lignin, despite being a hardwood species, is a direct result of its high G-lignin content. Additionally, minor amounts of other condensed linkages were observed in the MWL of leucaena, including β–β′ resinols (6 %) and β–1′ spirodienones (3 %), along with *p*-hydroxycinnamyl alcohol end-groups (5 %) and cinnamaldehydes (12 %). In contrast, tagasaste lignin, which had a slightly higher proportion of S-units, exhibited a higher proportion of β–*O*–4′ alkyl-aryl ether linkages, accounting for 74 % of all inter-unit linkages identified, and a lower content of condensed linkages, with β–5′ phenylcoumarans (11 %), β–β′ resinols (11 %), 5–5′ dibenzodioxocins (1 %), and β–1′ spirodienones (3 %). Additionally, the tagasaste lignin contained *p*-hydroxycinnamyl alcohol end-groups (4 %) and *p*-hydroxycinnamaldehydes (11 %).

3.5. Determination of aliphatic and phenolic hydroxyl groups by ^{31}P NMR spectroscopy

To gain a deeper understanding of the composition of the MWLs from leucaena and tagasaste, they were analyzed by ^{31}P NMR spectroscopy.

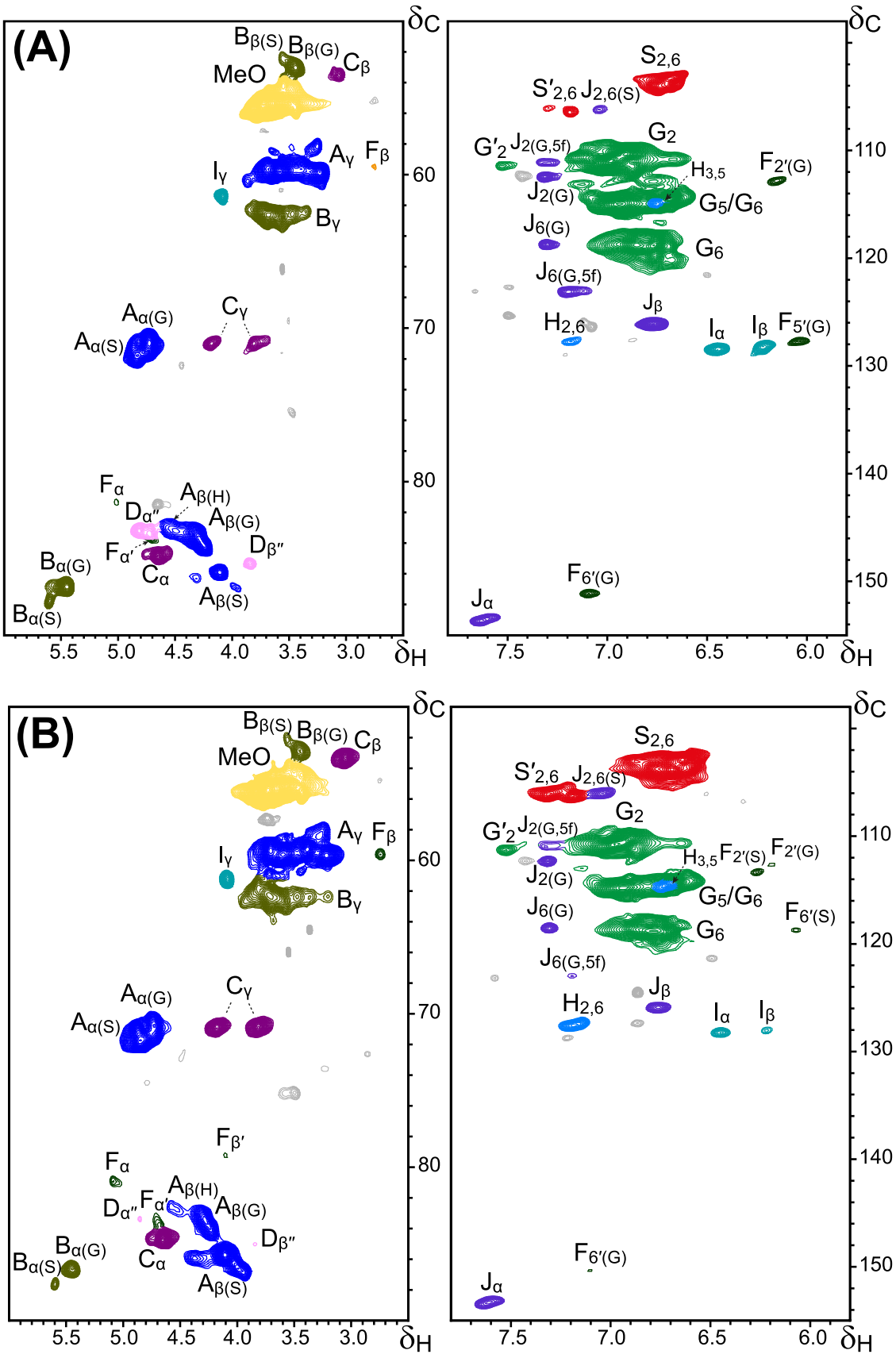

Fig. 3. Side-chain (δ_C/δ_H 50–90/2.5–6.0; left) and aromatic (δ_C/δ_H 98–155/5.8–7.8; right) regions of the HSQC spectra (in DMSO-d_6) of the MWLs isolated from leucaena (**A**) and tagasaste (**B**). The assignments of the different lignin correlation signals are listed in Table 4.

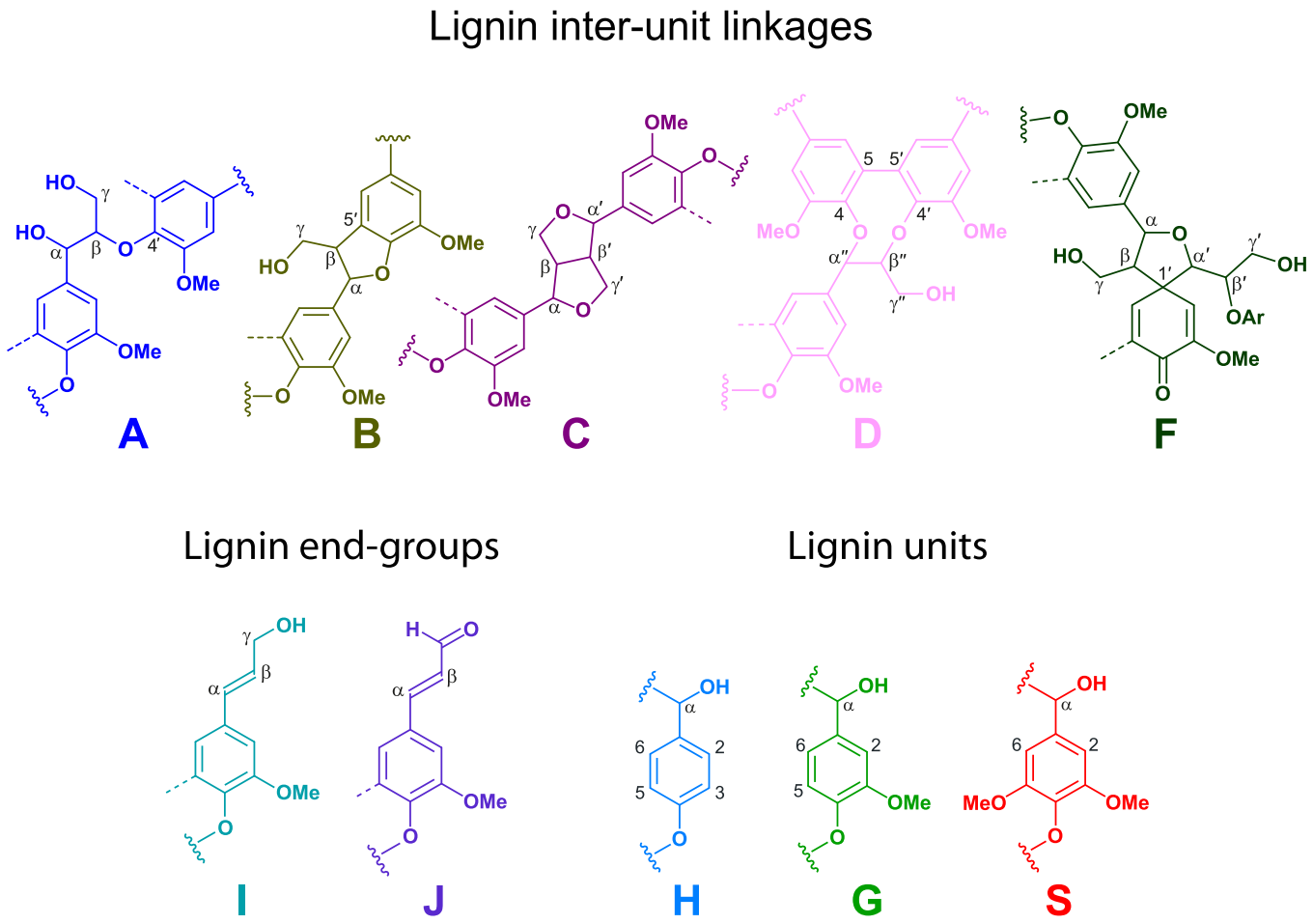

Fig. 4. Lignin structures identified in the HSQC spectra of the MWLs isolated from leucaena and tagasaste. **A**: β–*O*–4′ alkyl–aryl ethers; **B**: β–5′ phenylcoumarans; **C**: β–β′ resinols; **D**: 5–5′ dibenzodioxocins; **F**: β–1′ spirodienones; **I**: *p*-hydroxycinnamyl alcohol end-groups; **J**: *p*-hydroxycinnamaldehyde end-groups; **H**: *p*-hydroxyphenyl units; **G**: guaiacyl units; **G′**: α-oxidized guaiacyl units; **S**: syringyl units; **S′**: α-oxidized syringyl units.

This well-established NMR technique allows to differentiating and quantifying diverse hydroxyl groups within the lignin, including carboxylic, aliphatic, and phenolic groups (Pu et al., 2011; Meng et al., 2019). The ^{31}P NMR spectra of the MWLs from leucaena and tagasaste, along with the signal assignments for the main functional groups, are depicted in Fig. 5, while the corresponding quantitation data are summarized in Table 6.

In both samples, the dominant peaks in the ^{31}P NMR spectra were observed in the 145.0–150.0 ppm range and corresponded to the aliphatic hydroxyl groups on the lignin side-chains. These groups accounted for 4.87 mmol/g in the MWL of leucaena and 5.38 mmol/g in the MWL of tagasaste. Additionally, the spectra also revealed peaks between 137 and 145 ppm that are characteristics of phenolic hydroxyl groups derived from H, G, and S lignin units. In the MWL of leucaena, the phenolic hydroxyl content was 1.04 mmol/g, whereas in the MWL of tagasaste it was slightly lower at 0.80 mmol/g. Interestingly, the phenolics from G-lignin units were the most abundant in both MWLs, contributing 0.87 mmol/g in the MWL of leucaena and 0.52 mmol/g in the MWL of tagasaste, despite tagasaste having a predominance of S-units (S/G ratio of 1.13 according to 2D NMR). In contrast, phenolic hydroxyls from S-lignin units were detected in smaller amounts, accounting for 0.09 mmol/g in the MWL of leucaena and 0.19 mmol/g in the MWL of tagasaste. The H-lignin derived phenolics were present in trace amounts, at 0.08 and 0.09 mmol/g in the MWLs of leucaena and tagasaste, respectively. The low phenolic hydroxyl content is a typical feature of MWLs, primarily due to their gentle isolation under mild conditions, which preserves the native etherified structure of the plant lignin, in contrast to technical lignins, which are obtained through harsher chemical processes that extensively cleave bonds, leading to a significantly higher content of free phenolic hydroxyl groups (Pu et al., 2011). Finally, the carboxylic hydroxyl groups were observed in the 134.5–135.5 ppm range, albeit at lower intensities, corresponding to 0.16 mmol/g in the MWL of leucaena, and 0.15 mmol/g in the MWL of tagasaste.

3.6. *Anticipated performance of leucaena and tagasaste lignins in biorefinery applications*

Lignin content and composition are key factors for effectively utilizing lignocellulosic biomass in biorefineries. Lignin acts as a barrier to access the carbohydrates, such as cellulose, which are essential for producing valuable products like pulp, paper, bioethanol, and platform chemicals. Removing or modifying lignin is often necessary to expose these carbohydrates for further processing. However, lignin itself has considerable valorization potential due to its unique aromatic structure, which allows it to be transformed into a variety of bio-based chemicals, resins, and adhesives, making it a valuable resource on its own. Understanding the detailed lignin composition and structure is, therefore, essential for optimizing biomass conversion processes and maximizing the economic value of both the carbohydrates and the lignin in biorefineries. In the context of lignocellulosic biorefineries, this knowledge becomes even more crucial, as it allows for tailored strategies to enhance biomass processing efficiency and support the sustainable production of both energy and value-added materials. The distinct compositions and

Table 4
Assignments of the lignin $^{13}C/^{1}H$ correlation signals in the 2D HSQC spectra of the MWLs isolated from leucaena and tagasaste.

Label	δ_C/δ_H	Assignment
$B_{\beta(S)}$	52.3/3.57	C_β/H_β in phenylcoumarans (**B**) linked to S units
$B_{\beta(G)}$	53.0/3.45	C_β/H_β in phenylcoumarans (**B**) linked to G units
C_β	53.6/3.06	C_β/H_β in β–β′ resinols (**C**)
-OCH_3	55.5/3.72	C/H in methoxyls
A_γ	59.7/3.25 and 3.58	C_γ/H_γ in β–*O*–4′ alkyl-aryl ethers (**A**)
F_β	59.7/2.74	C_β/H_β in spirodienones (**F**)
I_γ	61.3/4.08	C_γ/H_γ in cinnamyl alcohol end-groups (**I**)
B_γ	62.5/3.67	C_γ/H_γ in phenylcoumarans (**B**)
C_γ	70.9/3.82 and 4.18	C_γ/H_γ in β–β′ resinols (**C**)
$A_{\alpha(G)}$	70.9/4.72	C_α/H_α in β–*O*–4′ alkyl-aryl ethers (**A**) linked to G units
$A_{\alpha(S)}$	71.9/4.85	C_α/H_α in β–*O*–4′ alkyl-aryl ethers (**A**) linked to S units
$F_{\beta'}$	79.3/4.11	$C_{\beta'}/H_{\beta'}$ in spirodienones (**F**)
F_α	81.0/5.09	C_α/H_α in spirodienones (**F**)
$A_{\beta(H)}$	82.7/4.58	C_β/H_β in β–*O*–4′ alkyl-aryl ethers (**A**) linked to H units
D_α	83.0/4.81	C_α/H_α in 5–5′ dibenzodioxocins (**D**)
$F_{\alpha'}$	83.4/4.70	$C_{\alpha'}/H_{\alpha'}$ in spirodienones (**F**)
$A_{\beta(G)}$	83.7/4.26	C_β/H_β in β–*O*–4′ alkyl-aryl ethers (**A**) linked to G units
C_α	84.8/4.66	C_α/H_α in β–β′ resinols (**C**)
D_β	85.3/3.83	C_β/H_β in 5–5′ dibenzodioxocins (**D**)
$A_{\beta(S)}$	85.8/4.09	C_β/H_β in β–*O*–4′ alkyl-aryl ethers (**A**) linked to S units
$B_{\alpha(G)}$	86.8/5.45	C_α/H_α in phenylcoumarans (**B**) linked to G units
$B_{\alpha(S)}$	87.8//5.61	C_α/H_α in phenylcoumarans (**B**) linked to S units
$S_{2,6}$	103.7/6.68	C_2/H_2 and C_6/H_6 in etherified syringyl units (**S**)
$J_{2,6(S)}$	106.1/7.04	C_2/H_2 and C_6/H_6 in sinapaldehyde end-groups (**J**)
$S'_{2,6}$	106.3/7.32 and 7.20	C_2/H_2 and C_6/H_6 in C_α-oxidized syringyl units (**S'**)
G_2	110.8/6.96	C_2/H_2 in guaiacyl units (**G**)
$J_{2(G,5f)}$	111.2/7.31	C_2/H_2 in coniferaldehyde end-groups C5-free (**J**)
G'_2	111.4/7.54	C_2/H_2 in C_α-oxidized guaiacyl units (**G'**)
$J_{2(G)}$	112.3/7.30	C_2/H_2 in coniferaldehyde end-groups C5-linked (**J**)
$F_{2'(G)}$	112.8/6.16	$C_{2'}/H_{2'}$ in guaiacyl spirodienones (**F**)
$F_{2(S)}$	113.5/6.27	$C_{2'}/H_{2'}$ in syringyl spirodienones (**F**)
G_5/G_6	115.0/6.74	C_5/H_5 and C_6/H_6 in guaiacyl units (**G**)
G_6	118.7/6.77	C_5/H_5 in guaiacyl units (**G**)
$J_{6(G)}$	118.7/7.30	C_6/H_6 in coniferaldehyde end-groups C5-linked (**J**)
$F_{6'(S)}$	118.8/6.08	$C_{6'}/H_{6'}$ in syringyl spirodienones (**F**)
$J_{6(G,5f)}$	123.0/7.19	C_6/H_6 in coniferaldehyde end-groups C5-free or β-*O*–4′ linked (**J**)
J_β	126.0/6.76	C_β/H_β in cinnamaldehyde end-groups (**J**)
$F_{5'(G)}$	127.6/6.04	$C_5/H_{5'}$ in guaiacyl spirodienones (**F**)
$H_{2,6}$	127.7/7.20	C_2/H_2 and C_6/H_6 in *p*-hydroxyphenyl units (**H**)
I_β	128.4/6.23	C_β/H_β in cinnamyl alcohol end-groups (**I**)
I_α	128.4/6.44	C_α/H_α in cinnamyl alcohol end-groups (**I**)
$F_{6'(G)}$	151.0/7.08	$C_{6'}/H_{6'}$ in guaiacyl spirodienones (**F**)
J_α	153.5/7.62	C_α/H_α in cinnamaldehyde end-groups (**J**)

Table 5
Structural characteristics (inter-unit linkages, *p*-hydroxycinnamyl end-groups, H-, G-, and S-lignin units, and S/G ratios) derived from integration of the signals in the HSQC of the MWLs from leucaena and tagasaste.

	MWL leucaena	MWL tagasaste
Lignin inter-unit linkages (%)		
β–*O*–4′ aryl ethers (**A**)	66	74
β–5′ Phenylcoumarans (**B**)	21	11
β–β′ Resinols (**C**)	6	11
5–5′ Dibenzodioxocins (**D**)	4	1
β–1′ Spirodienones (**F**)	3	3
Lignin end-groups[a]		
Cinnamyl alcohol end-groups (**I**)	5	4
Cinnamaldehyde end-groups (**J**)	12	11
Lignin aromatic units[b]		
H (%)	1	2
G (%)	83	46
S (%)	16	52
S/G ratio	0.19	1.13

[a] Expressed as a fraction of the total lignin inter-unit linkage types **A-F**
[b] Molar percentages (H+G+S=100)

structural characteristics of leucaena and tagasaste lignins offer opportunities to enhance biorefinery processes and develop new bio-based products.

In the case of carbohydrate valorization, both the overall lignin content and its composition play a crucial role in the efficiency of the delignification process. Guaiacyl (G) lignin, characterized by a higher proportion of condensed linkages, is more resistant to depolymerization in alkaline systems, such as the kraft process commonly used for cellulose pulp production, and exhibits lower reactivity compared to syringyl (S) lignin (Tsutsumi et al., 1995). In contrast, S-lignin is mainly composed of β–*O*–4′ ether linkages, which are more chemically labile and easier to break down. Consequently, lignocellulosic materials rich in G-lignin require higher alkali concentrations and harsher conditions compared to those with higher S/G lignin ratios (Tsutsumi et al., 1995; González-Vila et al., 1999; del Río et al., 2005; Santos et al., 2012; Li et al., 2016). Leucaena, with its high G-lignin composition, which promotes the formation of condensed linkages like phenylcoumarans and dibenzodioxocins, along with its relatively high lignin content (24.2 %), is expected to exhibit lower reactivity during alkaline delignification. This increased recalcitrance will require more severe processing conditions to effectively remove the lignin and access the carbohydrates (González-Vila et al., 1999; del Río et al., 2005; Santos et al., 2012; Li et al., 2016). In contrast, tagasaste, characterized by a higher lignin S/G ratio, a greater proportion of β–*O*–4′ alkyl-aryl ether linkages, fewer condensed linkages, and a lower overall lignin content (18.0 %), is expected to undergo delignification more easily. This facilitates better access to carbohydrates, making tagasaste more suitable for pulp and paper production, where easier delignification can reduce both energy and chemical consumption, as confirmed by previous studies (López et al., 2004, 2010; Domínguez-Robles et al., 2017, 2020).

When considering the valorization of the lignin fraction, its composition plays a crucial role in determining its potential applications. The G-unit-rich lignin in leucaena is particularly suited for producing phenols with unsubstituted C5 positions, which exhibit high reactivity making them ideal for synthesizing phenol-formaldehyde (PF) resins, making leucaena lignin valuable for such applications (de Menezes et al., 2017; Zhao et al., 2024). Moreover, leucaena lignin's G-unit structure and higher proportion of condensed linkages make it an excellent candidate for applications requiring durable and resistant materials (Gao et al., 2020; Kumar et al., 2021). Its distinctive structure could be particularly advantageous for producing high-performance composites, where it can enhance both mechanical properties and thermal stability (Gao et al., 2020; Kumar et al., 2021). Additionally, the high G-unit content of leucaena lignin provides a valuable source of vanillin and other G-derived compounds, which are in great demand in the food, fragrance, and pharmaceutical industries (S.S. Wang et al., 2017; Taher et al., 2023). In contrast, tagasaste is slightly enriched in S-lignin, which, due to its higher reactivity, is more suitable for catalytic conversion processes to produce valuable bio-based chemicals, such as fuels and monomers for polymer production (Constant et al., 2016; Gharehkhani et al., 2019; Tricker et al., 2020; Liu et al., 2022; Abu-Omar and Ford, 2023; Sun et al., 2024). Additionally, the higher abundance of β–*O*–4′ linkages in S-lignin contributes to its more linear structure (less branched), a key characteristic for producing high-performance carbon fibers. Its reduced cross-linking enhances spinnability, facilitating a more uniform carbonization process. This characteristic can lead to lower production costs and improved fiber quality, making S-lignin an attractive feedstock for advanced carbon fiber manufacturing (Li et al., 2021; Jia et al., 2023).

4. Conclusions

The lignin content, composition, and structure of two highly productive leguminous shrubs, leucaena and tagasaste, were thoroughly analyzed using different advanced analytical techniques. The results revealed significant differences in lignin content and composition

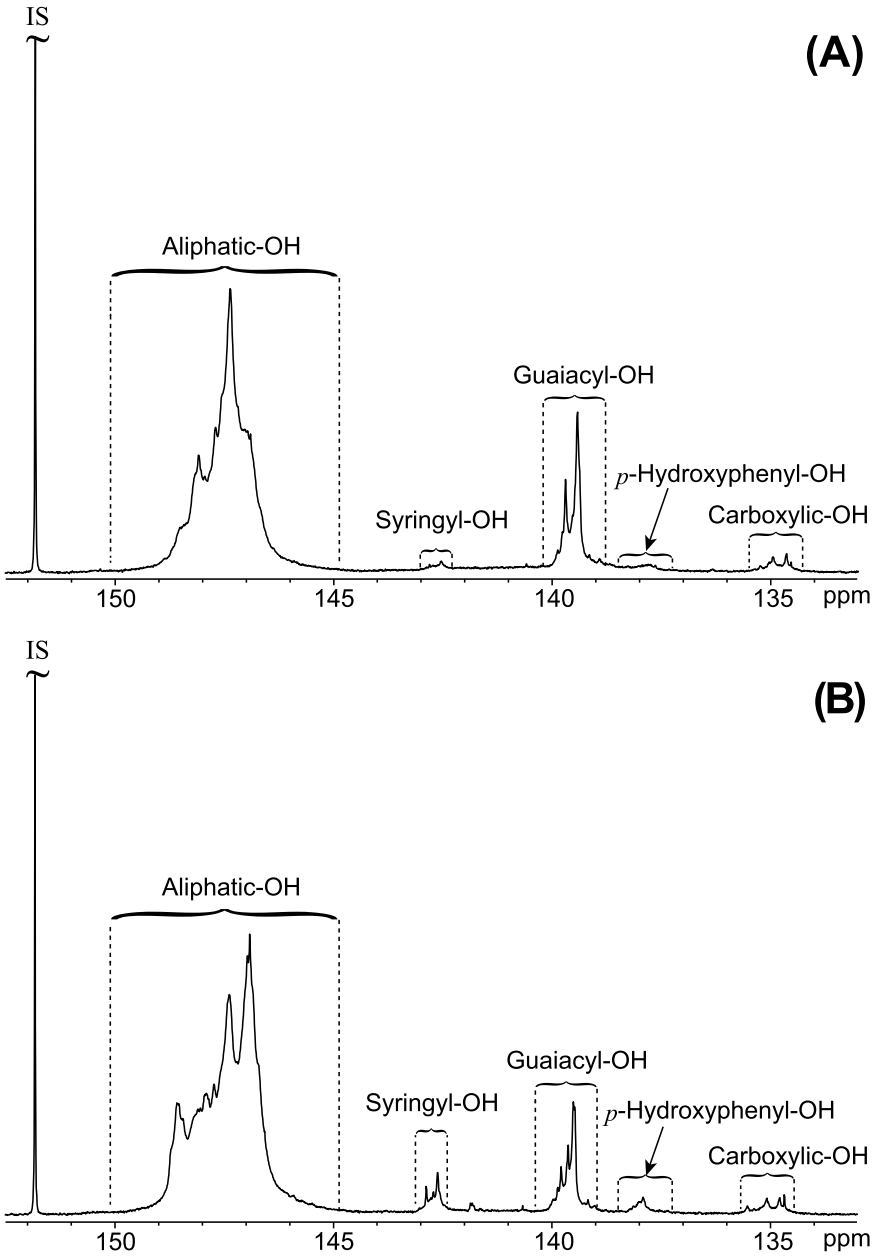

Fig. 5. ^{31}P NMR spectra of the MWLs isolated from leucaena (**A**) and tagasaste (**B**), phosphitylated with TMDP and using NHND as an internal standard (IS) for quantification. The identities and abundances (mmol OH/g lignin) of the different aliphatic, phenolic, and carboxylic hydroxyl groups, are indicated in Table 6.

Table 6
Quantitative analysis of aliphatic, phenolic (Syringyl + Guaiacyl + *p*-Hydroxyphenyl), and carboxylic hydroxyl group contents (mmol OH/g lignin) in the MWLs from leucaena and tagasaste, as determined by ^{31}P NMR spectroscopy.

	Content (mmol OH/g lignin)	
	MWL leucaena	MWL tagasaste
Aliphatic-OH	**4.87**	**5.38**
Phenolic-OH	**1.04**	**0.80**
H-OH	0.08	0.09
G-OH	0.87	0.52
S-OH	0.09	0.19
Carboxylic-OH	**0.16**	**0.15**

between the two leguminous plants. Leucaena exhibited a higher lignin content (24.2 %), with fewer β-ether linkages (66 % of all inter-unit linkages identified) and a greater prevalence of condensed linkages, which renders it less reactive during alkaline delignification. In contrast, tagasaste showed a lower lignin content (18.0 %), and a higher proportion of β-ether linkages (74 % of all inter-unit linkages identified) with fewer condensed linkages, indicating greater reactivity in such processes. These differences in lignin content composition could significantly influence their potential applications in lignocellulosic biorefineries. The study emphasizes the importance of accurately characterizing the native structure of lignins in lignocellulosic materials to select the most suitable methods or techniques for their effective valorization.

CRediT authorship contribution statement

del Río José Carlos: Writing – original draft, Validation,

Supervision, Resources, Methodology, Investigation, Funding acquisition, Data curation, Conceptualization. **Díaz Manuel J.:** Writing – review & editing, Resources, Investigation. **Gutiérrez Ana:** Writing – review & editing, Funding acquisition. **Rencoret Jorge:** Writing – review & editing, Methodology, Investigation, Funding acquisition, Formal analysis. **Rosado Mario J.:** Writing – review & editing, Resources, Methodology, Investigation, Formal analysis.

Declaration of Competing Interest

The authors declare that they have no known competing financial interests or personal relationships that could have appeared to influence the work reported in this paper

Acknowledgements

This work was financed by the Spanish Ministerio de Ciencia, Innovación y Universidades/Agencia Estatal de Investigación - MCIU/AEI/10.13039/501100011033, projects PID2020-118968RB-I00 and PID2023-152543OB-I00, the latter co-financed by the European Regional Development Fund (ERDF) "A way to make Europe". MJR acknowledges the Spanish Ministerio de Ciencia, Innovación y Universidades (MICIU) for a FPI fellowship (PRE2018-083267). The authors extend their sincere thanks to Dr. Manuel Angulo (CITIUS, University of Seville) for his invaluable support in the acquisition of the NMR spectra.

Data Availability

Data will be made available on request.

References

Abu-Omar, M.M., Ford, P.C., 2023. The lignin challenge in catalytic conversion of biomass solids to chemicals and fuels. RSC Sustain 1, 1686–1703. https://doi.org/10.1039/d3su00117b.

Alfaro, A., López, F., Pérez, A., García, J.C., Rodríguez, A., 2010. Integral valorization of tagasaste (*Chamaecytisus proliferus*) under hydrothermal and pulp processing. Bioresour. Technol. 101, 7635–7640. https://doi.org/10.1016/j.biortech.2010.04.059.

Benito, J., Marques, G., Rosado, M.J., Barro, F., Gutiérrez, A., del Río, J.C., Rencoret, J., 2024. Tritordeum, a hybrid cereal with a highly tricin-enriched lignin. Int. J. Biol. Macromol. 261, 129694. https://doi.org/10.1016/j.ijbiomac.2024.129694.

Björkman, A., 1956. Studies on finely divided wood. Part I. Extraction of lignin with neutral solvents. Sven. Papp. 59, 477–485.

Brosse, N., El Hage, R., Chaouch, M., Pétrissans, M., Dumarçay, S., Gérardin, P., 2010. Investigation of the chemical modifications of beech wood lignin during heat treatment. Polym. Degrad. Stab. 95, 1721–1726. https://doi.org/10.1016/j.polymdegradstab.2010.05.018.

Browning, B.L., 1967. Methods of wood chemistry; Wiley-Interscience. N. Y. https://doi.org/10.1002/pol.1968.160061112.

Constant, S., Wienk, H., Frissen, A., Peinder, P., Boelens, R., Es, D., Grisel, R., Weckhuysen, B., Huijgen, W., Gosselink, R., Bruijnincx, P., 2016. New insights into the structure and composition of technical lignins: a comparative characterisation study. Green. Chem. 18, 2651–2665. https://doi.org/10.1039/c5gc03043a.

de Menezes, F.F., Rencoret, J., Nakanishi, S.C., Nascimento, V.M., Silva, V.F.N., Gutiérrez, A., del Río, J.C., Rocha, G.J.M., 2017. Alkaline pretreatment severity leads to different lignin applications in sugar cane biorefineries. ACS Sustain. Chem. Eng. 5, 5702–5712. https://doi.org/10.1021/acssuschemeng.7b00265.

del Río, J.C., Gutiérrez, A., Hernando, M., Landín, P., Romero, J., Martínez, A.T., 2005. Determining the influence of eucalypt lignin composition in paper pulp yield using Py-GC/MS. J. Anal. Appl. Pyrol 74, 110–115. https://doi.org/10.1016/j.jaap.2004.10.010.

del Río, J.C., Gutiérrez, A., Martínez, M.J., Martínez, A.T., 2001. Py-GC/MS study of *Eucalyptus globulus* wood treated with different fungi. J. Anal. Appl. Pyrol 58 (59), 441–453. https://doi.org/10.1016/s0165-2370(00)00184-4.

del Río, J.C., Prinsen, P., Rencoret, J., Nieto, L., Jiménez-Barbero, J., Ralph, J., Martínez, A.T., Gutiérrez, A., 2012. Structural characterization of the lignin in the cortex and pith of elephant grass (*Pennisetum purpureum*) stems. J. Agric. Food Chem. 60, 3619–3634. https://doi.org/10.1021/jf300099g.

del Río, J.C., Speranza, M., Gutiérrez, A., Martínez, M.J., Martínez, A.T., 2002. Lignin attack during eucalypt wood decay by selected basidiomycetes: a Py-GC/MS study. J. Anal. Appl. Pyrol 64, 421–431. https://doi.org/10.1016/s0165-2370(02)00043-8.

Díaz, M.J., Alfaro, A., García, M.M., Eugenio, M.E., Ariza, J., Ló, F., 2004. Ethanol pulping from tagasaste (*Chamaecytisus proliferus* L.F. ssp palmensis) a new promising source for cellulose pulp. Ind. Eng. Chem. Res 43, 1875–1881. https://doi.org/10.1021/ie030611a.

Domínguez-Robles, J., Espinosa, E., Palenzuela, M.V., Eugenio, M.E., Rodríguez, A., Rosal, A., 2020. Evaluation of the potential of alternative vegetable materials for production of paper through kraft processes. Cell. Chem. Technol. 54, 73–81. https://doi.org/10.35812/cellulosechemtechnol.2020.54.08.

Domínguez-Robles, J., Sánchez, R., Espinosa, E., Savy, D., Mazzei, P., Piccolo, A., Rodríguez, A., 2017. Isolation and characterization of *Gramineae* and *Fabaceae* soda lignins. Int. J. Mol. Sci. 18, 327. https://doi.org/10.3390/ijms18020327.

Espinosa, E., Sánchez, R., González, Z., Domínguez-Robles, J., Ferrari, B., Rodríguez, A., 2017. Rapidly growing vegetables as new sources for lignocellulose nanofibre isolation: Physicochemical, thermal and rheological characterization. Carbohydr. Polym. 175, 27–37. https://doi.org/10.1016/j.carbpol.2017.07.055.

Feria, M.J., Alfaro, A., López, F., Pérez, A., García, J.C., Rivera, A., 2012. Integral valorization of *Leucaena diversifolia* by hydrothermal and pulp processing. Bioresour. Technol. 103, 381–388. https://doi.org/10.1016/j.biortech.2011.09.100.

Gao, S., Cheng, Z., Zhou, X., Liu, Y., Wang, J., Wang, C., Chu, F., Xu, F., Zhang, D., 2020. Fabrication of lignin based renewable dynamic networks and its applications as self-healing, antifungal and conductive adhesives. Chem. Eng. J. 394, 124896. https://doi.org/10.1016/j.cej.2020.124896.

García, M.M., Lopez, F., Alfaro, A., Ariza, J., Tapias, R., 2008. The use of tagasaste (*Chamaecytisus proliferus*) from different origins for biomass and paper production. Bioresour. Technol. 99, 3451–3457. https://doi.org/10.1016/j.biortech.2007.08.004.

Gharehkhani, S., Zhang, Y., Fatehi, P., 2019. Lignin-derived platform molecules through TEMPO catalytic oxidation strategies. Prog. Energy Combust. Sci. 72, 59–89. https://doi.org/10.1016/j.pecs.2019.01.002.

González, J.A., 2000. Estudio del tagasaste en el suroeste de España (Huelva). Diput. óN. De. Huelva, Huelva, Spain 145. ISBN: 8481632414.

González-Vila, F.J., Almendros, G., del Río, J.C., Martín, F., Gutiérrez, A., Romero, J., 1999. Ease of delignification assessment of wood from different *Eucalyptus* species by pyrolysis (TMAH)-GC/MS and CP/MAS ^{13}C NMR spectrometry. J. Anal. Appl. Pyrol 49, 295–305. https://doi.org/10.1016/s0165-2370(98)00097-7.

Jensen, E.S., Peoples, M.B., Boddey, R.M., Gresshoff, P.M., Hauggaard-Nielsen, H., Alves, B.J.R., Morrison, M.J., 2012. Legumes for mitigation of climate change and the provision of feedstock for biofuels and biorefineries. A review. Agron. Sustain. Dev. 32, 329–364. https://doi.org/10.1007/s13593-011-0056-7.

Jia, G., Innocent, M.T., Yu, Y., Hu, Z., Wang, X., Xiang, H., Zhu, M., 2023. Lignin-based carbon fibers: Insight into structural evolution from lignin pretreatment, fiber forming, to pre-oxidation and carbonization. Int. J. Biol. Macromol. 226, 646–659. https://doi.org/10.1016/j.ijbiomac.2022.12.053.

Jiménez, L., Pérez, A., de la Torre, M.J., Moral, A., Serrano, L., 2007. Characterization of vine shoots, cotton stalks, *Leucaena leucocephala* and *Chamaecytisus proliferus*, and of their ethyleneglycol pulps. Bioresour. Technol. 98, 3487–3490. https://doi.org/10.1016/j.biortech.2006.11.009.

Kamm, B., Gruber, P.R., Kamm, M., 2008. Biorefineries-Industrial Processes and Products: Status Quo and Future Directions. Wiley-VCH Verl. GmbH: Weinh., Ger. 2008.

Karhunen, P., Rummakko, P., Sipilä, J., Brunow, G., Kilpeläinen, I., 1995. Dibenzodioxocins; a novel type of linkage in softwood lignins. Tetrahedron Lett. 36, 169–170. https://doi.org/10.1016/0040-4039(94)02203-N.

Kumar, B., Agumba, D., Pham, D., Latif, M., Kim, D., Alrobei, H., Kim, J, H., 2021. Recent research progress on lignin-derived resins for natural fiber composite applications. Polymers 13, 1162. https://doi.org/10.3390/polym13071162.

Lago, C., Caldés, N., Lechón, Y., 2019. The Role of Bioenergy in the Emerging Bioeconomy - Resources, Technologies. Sustainability and Policy. Academic Press, London, UK.

Li, Q., Hu, C., Li, M., Truong, P., Li, J., Lin, H.-S., Naik, M.T., Xiang, S., Jackson, B.E., Kuo, W., Wu, W., Pu, Y., Ragauskas, A.J., Yuan, J.S., 2021. Enhancing the multifunctional properties of renewable lignin carbon fibers *via* defining the structure–property relationship using different biomass feedstocks. Green. Chem. 23, 3725–3739. https://doi.org/10.1039/d0gc03828h.

Li, M., Pu, Y., Ragauskas, A.J., 2016. Current understanding of the correlation of lignin structure with biomass recalcitrance. Front. Chem. 4, 45. https://doi.org/10.3389/fchem.2016.00045.

Liu, C., Luan, P., Li, Q., Cheng, Z., Xiang, P., Liu, D., Hou, Y., Yang, Y., Zhu, H., 2021. Biopolymers derived from trees as sustainable multifunctional materials: a review. Adv. Mater. 33, 2001654. https://doi.org/10.1002/adma.202001654.

Liu, B., Sanchez, M., Truong, J., Ford, P.C., Abu-Omar, M.M., 2022. Catalytic conversion of high S-lignin to a sustainable tri-epoxide polymer precursor. Green. Chem. 24, 4958–4968. https://doi.org/10.1039/d2gc01278b.

Loaiza, J.M., López, F., García, M.T., García, J.C., Díaz, M.J., 2017. Biomass valorization by using a sequence of acid hydrolysis and pyrolysis processes. Application to *Leucaena leucocephala*. Fuel 203, 393–402. https://doi.org/10.1016/j.fuel.2017.04.135.

Loaiza, J.M., López, F., García, M.T., García, J.C., Díaz, M.J., 2018. Integral valorization of tagasaste (*Chamaecytisus proliferus*) under thermochemical processes. Biomass-.-. Convers. Bior 8, 265–274. https://doi.org/10.1007/s13399-017-0258-6.

López, F., Alfaro, A., García, M.M., Díaz, M.J., Calero, A.M., Ariza, J., 2004. Pulp and paper from tagasaste (*Chamaecytisus proliferus* L.F. ssp *palmensis*). Chem. Eng. Res. Des. 82, 1029–1036. https://doi.org/10.1205/0263876041580730.

López, F., García, J.C., Pérez, A., Feria, M.J., Zamudio, M., Garrote, G., 2010. Chemical and energetic characterization of species with a high-biomass production: fractionation of their components. Environ. Prog. Sustain. Energy 29, 499–509. https://doi.org/10.1002/ep.10429.

Marques, G., Gutiérrez, A., del Río, J.C., 2008. Chemical composition of lignin and lipids from tagasaste (*Chamaecytisus proliferus* spp. *palmensis*). Ind. Crops Prod. 28, 29–36. https://doi.org/10.1016/j.indcrop.2007.12.007.

McKenzie, B.A., Hill, G.D., Ganeshan, V., Yamoah, E., Andrews, M.E., Humphry, D.R., 2001. The role of legumes in improving nitrogen availability, soil fertility and growth in the following crop. Asp. Appl. Biol. 63, 53–60.

Meng, X., Crestini, C., Ben, H., Hao, N., Pu, Y., Ragauskas, A.J., Argyropoulos, D.S., 2019. Determination of hydroxyl groups in biorefinery resources via quantitative ^{31}P NMR spectroscopy. Nat. Protoc. 14, 2627–2647. https://doi.org/10.1038/s41596-019-0191-1.

Monjardino, M., Revell, D., Pannell, D.J., 2010. The potential contribution of forage shrubs to economic returns and environmental management in Australian dryland agricultural systems. Agric. Syst. 103, 187–197. https://doi.org/10.1016/j.agsy.2009.12.007.

Nunes, L.J.R., Causer, T.P., Ciolkosz, D., 2020. Biomass for energy: a review on supply chain management models. Renew. Sustain. Energy Rev. 120, 109658. https://doi.org/10.1016/j.rser.2019.109658.

Palma, A., Loaiza, J.M., Díaz, M.J., García, J.C., Giráldez, I., López, F., 2021. Tagasaste, leucaena and paulownia: three industrial crops for energy and hemicelluloses production. Biotechnol. Biofuels Bioprod. 14, 89. https://doi.org/10.1186/s13068-021-01930-0.

Pu, Y., Cao, S., Ragauskas, A.J., 2011. Application of quantitative ^{31}P NMR in biomass lignin and biofuel precursors characterization. Energy Environ. Sci. 4, 3154–3166. https://doi.org/10.1039/c1ee01201k.

Ragauskas, A.J., Williams, C.K., Davison, B.H., Britovsek, G., Cairney, J., Eckert, C.A., Frederick, W.J., Hallett, J.P., Leak, D.J., Liotta, C.L., Mielenz, J.R., Murphy, R., Templer, R., Tschaplinski, T., 2006. The path forward for biofuels and biomaterials. Science 311, 484–489. https://doi.org/10.1126/science.1114736.

Ralph, J., Hatfield, R.D., 1991. Pyrolysis-GC-MS characterization of forage materials, 1991 J. Agric. Food Chem. 39, 1426–1437. https://doi.org/10.1021/jf00008a014.

Ralph, S.A., Landucci, L.L., Ralph, J., 2009. NMR Database of Lignin and Cell Wall Model Compounds. Available online: ⟨https://www.glbrc.org/databases_and_software/nmrdatabase⟩ (accessed on 29 April 2022).

Ralph, J., Lapierre, C., Boerjan, W., 2019. Lignin structure and its engineering. Curr. Opin. Biotechnol. 56, 240–249. https://doi.org/10.1016/j.copbio.2019.02.019.

Rencoret, J., Kim, H., Evaristo, A.B., Gutiérrez, A., Ralph, J., del Río, J.C., 2018. Variability in lignin composition and structure in cell walls of different parts of macaúba (*Acrocomia aculeata*) palm fruit. J. Agric. Food Chem. 66, 138–153. https://doi.org/10.1021/acs.jafc.7b04638.

Rodríguez-Echevarría, S., Pérez-Fernández, M.A., Vlaar, S., Finnan, T., 2003. Analysis of the legume-rhizobia symbiosis in shrubs from central western Spain. J. Appl. Microbiol 95, 1367–1374. https://doi.org/10.1046/j.1365-2672.2003.02118.x.

Rosado, M.J., Rencoret, J., Gutiérrez, A., del Río, J.C., 2023. Structural characterization of the milled-wood lignin isolated from sweet orange tree (*Citrus sinensis*) pruning residue. Polymers 15, 1840. https://doi.org/10.3390/polym15081840.

Santos, R.B., Lee, J.M., Jameel, H., Chang, H.-M., Lucia, L.A., 2012. Effects of hardwood structural and chemical characteristics on enzymatic hydrolysis for biofuel production. Bioresour. Technol. 110, 232–238. https://doi.org/10.1016/j.biortech.2012.01.085.

Stagnari, F., Maggio, A., Galieni, A., Pisante, M., 2017. Multiple benefits of legumes for agriculture sustainability: an overview. Chem. Biol. Technol. Agric. 4, 2. https://doi.org/10.1186/s40538-016-0085-1.

Sun, P., Wang, Z., Li, C., Tang, B., Peng, C., 2024. Catalytic conversion of lignin and its derivatives to alkanes over multifunctional catalysts: A review. Fuel 361, 130726. https://doi.org/10.1016/j.fuel.2023.130726.

Taher, M., Wang, X., Hasan, F., Miah, M., Zhu, J., Chen, J., 2023. Lignin modification for enhanced performance of polymer composites. ACS Appl. Bio Mater. 6, 5169–5192. https://doi.org/10.1021/acsabm.3c00783.

Tappi, 2004. Tappi Test Methods 2004-2005. Tappi Press, Norcoss, GA, USA.

Tolbert, A., Akinosho, H., Khunsupat, R., Naskar, A.K., Ragauskas, A.J., 2014. Characterization and analysis of the molecular weight of lignin for biorefining studies. Biofuels Bioprod. Biorefin 8, 836–856. https://doi.org/10.1002/bbb.1500.

Tricker, A., Stellato, M., Kwok, T., Kruyer, N., Wang, Z., Nair, S., Thomas, V., Realff, M., Bommarius, A., Sievers, C., 2020. Similarities in recalcitrant structures of industrial non-kraft and kraft lignin. ChemSusChem 13, 4624–4632. https://doi.org/10.1002/cssc.202001219.

Tsutsumi, Y., Kondo, R., Sakai, K., Imamura, H., 1995. The difference of reactivity between syringyl lignin and guaiacyl lignin in alkaline systems. Holzforschung 49, 423–428. https://doi.org/10.1515/hfsg.1995.49.5.423.

Ubando, A.T., Felix, C.B., Chen, W.-H., 2020. Biorefineries in circular bioeconomy: A comprehensive review. Bioresour. Technol. 299, 122585. https://doi.org/10.1016/j.biortech.2019.122585.

Vanholme, R., Demedts, B., Morreel, K., Ralph, J., Boerjan, W., 2010. Lignin biosynthesis and structure. Plant Physiol. 153, 895–905. https://doi.org/10.1104/pp.110.155119.

Vinod, A., Sanjay, M.R., Suchart, S., Jyotishkumar, P., 2020. Renewable and sustainable biobased materials: An assessment on biofibers, biofilms, biopolymers and biocomposites. J. Clean. Prod. 258, 120978. https://doi.org/10.1016/j.jclepro.2020.120978.

Wang, H.M., Wang, B., Wen, J.L., Yuan, T.Q., Sun, R.C., 2017. Structural characteristics of lignin macromolecules from different Eucalyptus species. ACS Sustain. Chem. Eng. 5, 11618–11627. https://doi.org/10.1021/acssuschemeng.7b02970.

Wang, S.S., Xu, C., Liu, Y., Dai, J., Wang, Z., Liu, X., Chen, J., Shen, X., Wei, J., Zhu, J., 2017. Vanillin-derived high-performance flame retardant epoxy resins: facile synthesis and properties. Macromolecules 50, 1892–1901. https://doi.org/10.1021/acs.macromol.7b00097.

Wu, G.-L., Liu, Y., Tian, F.-P., Shi, Z.-H., 2017. Legumes functional group promotes soil organic carbon and nitrogen storage by increasing plant diversity. Land Degrad. Dev. 28, 1336–1344. https://doi.org/10.1002/ldr.2570.

Yang, L., Wang, X.-C., Dai, M., Chen, B., Qiao, Y., Deng, H., Zhang, D., Zhang, Y., de Almeida, C.M.V.B., Chiu, A.S.F., Klemeš, J.J., Wang, Y., 2021. Shifting from fossil-based economy to bio-based economy: Status quo, challenges, and prospects. Energy 228, 120533. https://doi.org/10.1016/j.energy.2021.120533.

Zhao, L., Li, W., Cheng, Y., Zhao, J., Tian, D., Huang, M., Shen, F., 2024. Preparation and evaluation of lignin-phenol-formaldehyde resin as wood adhesive using unmodified lignin. Ind. Crops Prod. 211, 118168. https://doi.org/10.1016/j.indcrop.2024.118168.